Neoplasma 2026; 73(1): 26–36

doi:10.4149/neo_2025_250518N209

SLC44A1 promotes AML progression and chemoresistance by regulating the Notch signaling pathway

Shuyun CAO[1,2,3], Chengyun PAN[1,3], Xiuying HU[1,2,3], Tianzhen HU[1,3,4], Yanju LI[1,3], Qin FANG[5], Jishi WANG[1,2,3,4,6,*]

[1]Department of Hematology, Affiliated Hospital of Guizhou Medical University, Guiyang, China; [2]School of Clinical Medicine, Guizhou Medical University, Guiyang, China; [3]Province Institute of Hematology, Guiyang, China; [4]Guizhou Province Hematopoietic Stem Cell Transplantation Centre and Key Laboratory of Hematological Disease Diagnostic and Treatment Centre, Guiyang, China; [5]Department of Pharmacy, Affiliated Hospital of Guizhou Medical University, Guiyang, China; [6]National Clinical Research Center for Hematologic Diseases, The First Affiliated Hospital of Soochow University, Soochow, China

**Correspondence: wangjishi9646@163.com*

Received May 18, 2025 / Accepted December 22, 2025

Despite advances in treatment, acute myeloid leukemia (AML) remains a formidable therapeutic challenge, highlighting the urgent need for novel biomarkers and therapeutic targets. The choline transporter SLC44A1 has been implicated in cancer progression; however, its role in AML remains largely unexplored. Here, we investigated the clinical relevance and molecular mechanisms of SLC44A1 in AML. Analysis of The Cancer Genome Atlas (TCGA) datasets revealed significant upregulation of SLC44A1 in AML patients, correlating with poor patient prognosis. Functional studies demonstrated that SLC44A1 knockdown markedly inhibited AML cell proliferation and enhanced chemosensitivity to cytarabine and venetoclax. RNA sequencing and pathway analysis identified the NOTCH signaling pathway as a key downstream target of SLC44A1, which was further validated by western blot. Collectively, our findings establish SLC44A1 as a crucial regulator of AML progression and chemoresistance, highlighting its dual potential as a prognostic biomarker and a therapeutic target.

Key words: SLC44A1; acute myeloid leukemia; proliferation; chemoresistance; Notch signaling

Acute myeloid leukemia (AML) is a hematological malignancy derived from hematopoietic stem cells and progenitor cells, and it represents the most prevalent type of leukemia in adults, with a median age of onset of 68 years [1]. Over recent decades, the treatment paradigm for AML has evolved from standard chemotherapy regimens, such as the "3+7" protocol, to novel targeted therapies, including venetoclax and sorafenib, among others [2]. Despite improvements in prognosis, the survival rate for patients over 65 years old remains low, with a persistent risk of relapse and refractory disease [3]. This underscores the urgent need for novel biomarkers to enhance diagnostic accuracy, predict survival outcomes, and guide therapeutic strategies.

The solute carrier family 44 (SLC44) proteins, also known as choline transporter-like proteins, are involved in choline metabolism and have been implicated in cancer progression [4]. Choline accumulation in tumors is mediated by SLC44, increasing the cell membrane synthesis during active cell proliferation in several cancer types [5–7]. Among them, SLC44A1 plays a crucial role in choline transport across the plasma and mitochondrial membranes, supporting synthesis pathways essential for cell growth [8]. Notably, emerging evidence suggests that SLC44A1 is involved in tongue squamous cell carcinoma, small cell lung carcinoma, pancreatic cancer cell proliferation, migration, and metastasis [9–11]. However, its role in AML remains largely unexplored.

In this study, we investigated the expression levels of *SLC44A1* in AML and examined its association with clinicopathological features and patient prognosis. Additionally, we conducted cellular experiments to elucidate the underlying mechanisms by which SLC44A1 contributes to AML progression and chemoresistance. Our study evaluates the potential of SLC44A1 as a diagnostic marker and therapeutic target in AML.

Patients and methods

Gene expression analysis. The TIMER 2.0 [12] website (https://compbio.cn/timer2/) and the Gene Expression Profiling Interactive Analysis (GEPIA) [13] platform (http://

gepia.cancer-pku.cn/) were employed to analyze the expression of the SLC44 family in pan-cancer compared to normal tissues. The Gene Expression Omnibus (GEO) database [14] (https://www.ncbi.nlm.nih.gov/geo/) was used for external validation. Data from the GSE103424 dataset [15] was analyzed to evaluate differential SLC44A1 expression patterns in relation to treatment response. Data obtained from The Cancer Genome Atlas (TCGA) [16] (https://tcga-data.nci.nih.gov/tcga/) and the Genotype-Tissue Expression (GTEx) [17] (https://gtexportal.org/home) databases were used to explore the correlations between SLC44A1 expression levels, clinicopathological parameters, and prognosis. Additionally, LinkedOmics [18] (http://www.linkedomics.org/login.php) was utilized to investigate associations between SLC44A1 expression and molecular features. Based on the GSE116256 [19] dataset, SLC44A1 levels within single-cell data were displayed by the "Nebulosa" R package. Differential SLC44A1 expression in diverse cells was analyzed with the "Libra" package. The relationships of SLC44A expression with cancerous hematopoietic cells in certain differentiation stages were provided by BloodSpot [20] (https://www.fobinf.com/).

Patient samples and cell lines. A total of 28 bone marrow specimens were collected from patients with AML and healthy donors at the Affiliated Hospital of Guizhou Medical University between 2022 and 2023 using simple random sampling. Clinical characteristics of patients are summarized in Supplementary Table S1. Bone marrow mononuclear cells from AML patients and healthy donors were isolated by Ficoll density gradient centrifugation. This study was approved by the Institutional Research Ethics Committee, and written informed consent was obtained from all participants.

The human AML cells (THP1 and MV4-11) were obtained from the ATCC (American Type Culture Collection, USA) and authenticated before use. Cells were cultured in a medium supplemented with 10% certified heat-inactivated fetal bovine serum (FBS; SAFC Bioscience, Lenexa, KS, USA) and penicillin (Sigma Life Sciences, St. Louis, MO, USA) and incubated at 37 °C with 5% CO_2.

Immunofluorescence. Cells were fixed in 4% paraformaldehyde (4 °C, overnight), then washed with PBS (×3). Permeabilization was performed with Triton X-100 (15 min), followed by PBS washes (×3). After blocking with goat serum (1 h), cells were incubated with anti-SLC44A1 primary antibody (1:200, 4 °C, 24 h) and washed (PBS, ×3). A CoraLite594-conjugated secondary antibody (1:100, 1 h) was applied. Nuclei were counterstained with DAPI, and images were acquired using an Olympus BX51 fluorescence microscope.

Lentiviral transfection. The SLC44A1-silencing RNA (shSLC44A1) was acquired from Genechem Co., Ltd. (Shanghai, China). Following specific instructions, we transfected the empty vector and SLC44A1-shRNA into the THP-1 and MV4-11 cells. The shRNA sequence for SLC44A1 was 5'-GAGCAGCTTCAGATAGCTGAA-3'. The sequence for the control shRNA was 5'-TTCTCCGAACGTGTCACGT-3'. A Western blot was used to determine the transfection efficiency. Lentivirus-infected cells were selected with puromycin at a final concentration of 3 μg/ml for THP-1 cells and 2 μg/ml for MV4-11 cells.

Western blot. A radioimmunoprecipitation (RIPA) lysis buffer that contained 1% phenylmethylsulfonyl fluoride (PMSF) (Solarbio Science & Technology, Beijing, China) was added to extract the total cellular proteins under 30 min of agitation. After this, extracts were collected by centrifugation for 15 minutes at 12,000×g and 4 °C to obtain the supernatants. Subsequently, a bicinchoninic acid (BCA) kit (Solarbio, China) was used to detect the protein content. The 20 μg proteins were later isolated by loading on 10% SDS-PAGE before being transferred onto polyvinylidene difluoride (PVDF) membranes at 120 V/250 mA. Subsequently, the membrane was blocked by 5% nonfat milk for two hours. This was followed by another two hours of incubation with primary antibody SLC44A1 (#14687-1-AP 1:1000); β-actin (#K006153P 1:1000); NOTCH2 (#ERP26111-69 1:1000); APH1A (#YN6455 1:1000) at ambient temperature or overnight incubation at 4 °C. Moreover, the HRP-labeled Affinipure Goat Anti-Rabbit IgG secondary antibody (H + L) was utilized. An electrochemiluminescence (ECL) kit (4 A Biotech, China) was used to investigate the protein bands, and ImageJ was used for the quantification.

Cell viability assay. Cells were seeded (2×10^3/well) onto 96-well plates for 1, 3, 5 days, and the cell viability was evaluated using the Cell Counting Kit-8 (CCK-8, Target Molecule Corp, China). A microplate ultra-micro spectrophotometer was used to evaluate the absorbance at 450 nm.

Drug sensitivity assay. For chemosensitivity evaluation, cells were plated at 1×10^4 cells/well in 96-well plates and exposed to gradient concentrations of venetoclax (0, 2, 4, 8 nM for MV4-11 cells; 0, 50, 150, 200 nM for THP1 cells) and cytarabine (0, 0.25, 0.5, 1 μM for MV4-11 and THP1 cells) for 24 h. Following drug treatment, cell viability was quantified using the CCK-8 assay described above. The proportion of apoptotic cells was determined using the Annexin V-APC/7-AAD Apoptosis Kit (MultiSciences, China) according to the manufacturer's protocol. Cells were plated in 6-well plates at a density of 1×10^5 cells/well and treated with drugs for 24 h, then analyzed on a FACSCalibur instrument (BD Biosciences, San Jose, CA, USA).

EdU incorporation assay. In accordance with the manufacturer's instructions, the cell-Light™ EdU Apollo567 In Vitro Kit (#C10310-1, Ribobio, China) was used for the EdU incorporation assay.

RNA-sequencing analysis. Total cellular RNA was extracted using the TRIzol reagent kit (Invitrogen, Carlsbad, CA, USA). RNA quality was evaluated with the Agilent 2100 Bioanalyzer (Agilent Technologies, Santa Clara, CA, USA). Sequencing libraries were prepared using the NEBNext Ultra RNA Library Prep Kit for Illumina (#E7770, New England Biolabs, Ipswich, MA, USA). RNA sequencing was performed on the Illumina NovaSeq 6000 platform by

Gene Denovo Biotechnology Co. (Guangzhou, China). Read quality was assessed using FastQC, and gene expression levels were quantified with RSEM. Differentially expressed genes were identified based on thresholds of FDR <0.05 and $|\log_2$ fold change (FC)| >2. The raw sequencing data have been deposited in the National Center for Biotechnology Information (NCBI) repository under the accession number PRJNA1223631.

Statistical analyses. The Shapiro-Wilk test was used to check whether the continuous variables of the different groups conformed to normal distributions. Non-normally distributed data were explored using the Wilcoxon rank-sum test, or they were compared using the Mann-Whitney U test or Student's t-test. A chi-square test or Fisher's exact test was utilized to compare the categorical variables. A one-way analysis of variance (ANOVA) was employed to evaluate statistical differences among multiple groups. R software (version 4.3.1) was used for the analyses. A p-value <0.05 (two-tailed) was statistically significant.

Results

SLC44A1 expression in pan-cancer. We initiated our investigation with a comprehensive pan-cancer analysis of the SLC44 protein family, which revealed that SLC44A1 exhibited the most prominent upregulation across multiple malignancies (Supplementary Figures S1A, S1B). This finding prompted us to focus specifically on SLC44A1 for subsequent analyses. Through systematic evaluation using the TIMER 2.0 platform and the GEPIA database, we compared SLC44A1 expression profiles between tumor and adjacent normal tissues across 33 cancer types derived from TCGA. Notably, among all SLC44 family members, SLC44A1 demonstrated significantly elevated expression in 14 distinct cancer types, including bladder urothelial carcinoma (BLCA), breast invasive carcinoma (BRCA), cervical squamous cell carcinoma (CESC), cholangiocarcinoma (CHOL), colon adenocarcinoma (COAD), esophageal carcinoma (ESCA), head and neck squamous cell carcinoma (HNSC), lung adenocarcinoma (LUAD), lung squamous cell carcinoma (LUSC), stomach adenocarcinoma (STAD), diffuse large B-cell lymphoma (DLBC), acute myeloid leukemia (AML), lower-grade glioma (LGG), and testicular germ cell tumors (TGCT). SLC44A1 protein levels were elevated in solid tumors, including BRCA, CCRCC, UCEC, PAAD, and HNSC. In contrast, its expression was reduced in COAD, OV, RCC, GBM, liver cancer (LC), and lung cancer (Supplementary Figure S1C).

Comprehensive evaluation of SLC44A1 expression in AML. A comprehensive pan-cancer analysis revealed that SLC44A1 exhibited the most pronounced overexpression in AML relative to normal controls, prompting our subsequent evaluation of its clinical relevance in AML patients. The cohort consisted of 173 adult patients from TCGA dataset, categorized into two groups based on the median SLC44A1 expression level, with their clinicopathological characteristics summarized in Table 1. Patients in the SLC44A1^{high} group exhibited elevated white blood cell (WBC) counts and were more frequently associated with non-M3 subtypes, particularly M4 and M5, according to the FAB classification. Additionally, the SLC44A1high group exhibited a higher prevalence of NPM1 and FLT3 mutations, as well as a poorer cytogenetic risk profile (Table 1).

SLC44A1 expression was significantly elevated in patients with high tumor burden (WBC≥10×10^9/l) compared to those with lower WBC counts (Supplementary Figure S2A). Furthermore, SLC44A1 was markedly upregulated in the poor cytogenetic risk group versus the favorable-risk cohort (Supplementary Figure S2B). Notably, acute promyelocytic leukemia (APL) subtypes displayed higher SLC44A1 expression than non-APL cases (Supplementary Figure S2C). Further classification of patients based on the FAB subtypes revealed that SLC44A1 expression was highest in the M5 subtype, followed by the M4 subtype (Supplementary Figure S2D). FLT3 and DNMT3A mutations are known to be associated with poor prognosis in AML patients [21], data from the LinkedOmics database indicated that SLC44A1 expression was markedly elevated in patients with DNMT3A mutation (R882H) (Supplementary Figure S2E), FLT3 mutation (D835Y) (Supplementary Figure S2F), and NPM1 mutation (W288F) (Supplementary Figure S2G) at the mRNA level. It should be noted that the prognostic significance of isolated NPM1 mutations in favorable-risk AML patients remains limited. According to a previous study [22], a comprehensive prognostic evaluation must incorporate both FLT3 mutational analysis and contemporary risk stratification criteria. Furthermore, ROC analysis of TCGA cohort revealed perfect diagnostic discrimination (AUC=1.0) for SLC44A1 in AML (Supplementary Figure S2H). To evaluate differential SLC44A1 expression patterns associated with treatment response, we analyzed the GSE103424 dataset comprising 36 *de novo* AML samples, stratified into complete remission (CR) and non-complete remission (non-CR) groups based on their response to the standard "7+3" induction regimen (cytarabine plus daunorubicin). Notably, our analysis revealed significantly higher SLC44A1 expression levels in the non-CR group compared to the CR group (Supplementary Figure S2I) in our center. These results indicate that SLC44A1 could be a promising candidate for further investigation as a diagnostic biomarker in AML.

SLC44A1 correlates with poor prognosis in AML patients. In TCGA cohort, high SLC44A1 expression was associated with poorer overall survival (OS; p<0.001, Supplementary Figure S3A) and event-free survival (EFS; p<0.001, Supplementary Figure S3B). Even within the good/intermediate-risk groups, the SLC44A1^{high} group demonstrated significantly worse OS (p=0.00373, Supplementary Figure S3C) and EFS (p=0.0168, Supplementary Figure S3D).

Using univariate analysis (Table 2), age ≥60 years (p<0.001), *FLT3* mutation (p=0.039), *DNMT3A* mutation

Table 1. Clinicopathological features of the AML patients in TCGA cohort.

Characteristics	Overall (n=173)	SLC44A1^{low} (n=86)	SLC44A1^{high} (n= 87)	p-value
Sex (%)				0.197
Male	93 (53.8%)	42 (48.8%)	51 (58.6%)	
Female	80 (46.2%)	44 (51.2%)	36 (41.4%)	
Age (median [IQR])	58 [46–68]	59 [41–67]	58 [44–67]	0.787
WBC count (×10^9/l) (median [IQR])	18.5 [3.25–58.5]	10 [2–42.5]	30 [8–73]	0.001
BM blasts (%) (median [IQR])	48 [16–48]	53 [18–80]	47 [11–66]	0.201
PB blasts (%) (median [IQR])	71.5 [51–85.75]	69 [48–85]	72 [52–86]	0.525
FAB classifications (%)				0.002
M0	16 (9.2%)	12 (14.1%)	4 (4.7%)	
M1	42 (24.3%)	21 (24.7%)	21 (24.4%)	
M2	39 (22.5%)	20 (23.5%)	19 (22.1%)	
M3	16 (9.2%)	12 (14.1%)	4 (4.7%)	
M4	35 (20.2%)	14 (16.5%)	21 (24.4%)	
M5	18 (10.4%)	2 (2.4%)	16 (18.6%)	
M6	2 (1.2%)	2 (2.4%)	0 (0.00%)	
M7	3 (1.7%)	2 (2.4%)	1 (1.2%)	
FLT3 mutation (%)				0.032
Wild	124 (71.7%)	68 (79.1%)	56 (64.4%)	
Mutated	49 (28.3%)	18 (20.9%)	31 (35.6%)	
DNMT3A mutation (%)				
Wild	130 (75.1%)	70 (81.4%)	60 (69.0%)	0.059
Mutated	43 (24.9%)	16 (18.6%)	27 (31.0%)	
RUNX1 mutation (%)				0.583
Wild	157 (90.8%)	77 (89.5%)	80 (92.0%)	
Mutated	16 (9.2%)	9 (10.5%)	7 (8.0%)	
NPM1 mutation (%)				0.008
Wild	125 (72.3%)	70 (81.4%)	55 (63.2%)	
Mutated	48 (27.7%)	16 (18.6%)	32 (36.8%)	
IDH1 mutation (%)				0.583
Wild	157 (90.8%)	77 (89.5%)	80 (92.0%)	
Mutated	16 (9.2%)	9 (10.5%)	7 (8.0%)	
RAS mutation (%)				0.234
Wild	154 (89.0%)	79 (91.9%)	75 (86.2%)	
Mutated	19 (11.0%)	7 (8.1%)	12 (13.8%)	
Risk level (%)				
Good	32 (18.7%)	26 (30.6%)	6 (7.0%)	<0.001
Intermediate	103 (60.2%)	38 (44.7%)	65 (75.6%)	
Poor	36 (21.1%)	21 (24.7%)	15 (17.4%)	

(p=0.012), *RUNX1* mutation (p=0.047), intermediate/poor risk level (p<0.001), and high SLC44A1 expression (p=0.011) were associated with inferior OS. Consistently, WBC count ≥10×10^9/l (p=0.004), *FLT3* mutation (p=0.035), intermediate/poor risk level (p<0.001), and high SLC44A1 expression (p=0.047) were associated with inferior EFS (Table 2). However, multivariate analysis revealed that age ≥60 was the only independent risk factor for both OS and EFS (p<0.001).

Based on the multivariate Cox analysis, a predictive nomogram was constructed to estimate 1-, 3-, and 5-year OS and EFS (Supplementary Figures S2G, S2H). The area under the curve (AUC) values for the nomogram were 0.799, 0.823, and 0.878 for 1-, 3-, and 5-year OS, respectively (Supplementary Figure S3E), and 0.773, 0.732, and 0.894 for 1-, 3-, and 5-year EFS, respectively (Supplementary Figure S3F), demonstrating robust predictive specificity and sensitivity.

Stage-specific expression pattern of SLC44A1 in hematopoietic differentiation and validation in single-cell data. BloodSpot analysis revealed stage-specific SLC44A1 expression patterns in hematopoietic differentiation, showing predominant expression in promonocytes (Supplementary Figure S4A). This observation was validated by the

Table 2. Univariate analysis for OS and EFS.

Characteristics	Overall survival (OS)			Event-free survival (EFS)		
	HR	95% CI	p-value	HR	95% CI	p-value
Age (≥60 vs. <60)	3.221	2.146–4.832	<0.001	1.834	1.729–3.647	<0.001
Sex (female vs. male)	1.008	0.676–1.503	0.97	0.912	0.674–1.422	0.912
WBC count (≥15 vs. < 15×10^9/l)	1.434	0.959–2.145	0.079	1.745	1.194–2.55	0.004
BM blasts (≥70% vs.<70%)	1.187	0.795–1.772	0.403	1.14	0.785–1.653	0.492
PB blasts (≥30% vs. <30%)	1.135	0.755–1.707	0.542	1.448	0.984–2.131	0.06
FLT3 (mutated vs. wild)	1.574	1.024–2.422	0.039	1.537	1.031–2.292	0.035
NPM1 (mutated vs. wild)	1.142	0.728–1.79	0.564	1.106	0.728–1.628	0.636
DNMT3A (mutated vs. wild)	1.775	1.133–2.781	0.012	1.469	0.962–2.242	0.075
IDH1 (mutated vs. wild)	0.785	0.38–1.619	0.511	0.827	0.431–1.584	0.566
RUNX1 (mutated vs. wild)	1.464	1.005–2.133	0.047	1.427	0.782–2.605	0.247
NRAS (mutated vs. wild)	0.526	0.166–1.665	0.275	0.918	0.374–2.254	0.853
KRAS (mutated vs. wild)	1.745	0.763–3.991	0.187	1.979	0.919–4.264	0.081
Risk (intermediate/poor vs. good)	1.745	1.834–6.884	<0.001	2.88	1.638–5.063	<0.001
SLC44A1 (high vs. low)	1.7	1.131–2.554	0.011	1.834	1.834–2.133	0.047

single-cell RNA sequencing data analysis (Supplementary Figures S4B, S4C), consistent with our previous finding of SLC44A1 overexpression in FAB-M4/M5 AML subtypes.

Knockdown of SLC44A1 decreased AML cell proliferation. Immunofluorescence staining confirmed the expression of SLC44A1 in M4/M5-representative cell lines (THP-1 and MV4-11) and primary AML samples, revealing its dual nuclear and cytoplasmic localization (Figure 1A). Consistent with this, an initial analysis of our institutional cohort revealed that SLC44A1 expression was significantly elevated in AML patients compared to healthy controls, at both the protein (Figures 1B and 1C) and mRNA levels (Figure 1D). To further investigate the functional role of SLC44A1 in AML, we knock down SLC44A1 by lentivirus infection (Figure 1E). CCK-8 and the EdU incorporation assays were performed to evaluate the effect of SLC44A1 on AML cell proliferation. CCK-8 assay was performed to evaluate the effect of SLC44A1 on AML cell viability (Figures 1F, 1G). In parallel, the EdU incorporation assays were utilized to assess the effect of SLC44A1 on AML cell proliferation (Figures 1H–1K). The results demonstrated that the knockdown of SLC44A1 significantly suppressed the proliferation of MV4-11 and THP1 cells. These findings suggested that SLC44A1 plays a critical role in promoting AML cell proliferation.

SLC44A1 regulated the therapeutic efficacy of AML. Bioinformatics analysis revealed elevated SLC44A1 expression in AML patients who failed to achieve CR following conventional chemotherapy regimens, suggesting a potential association between SLC44A1 and chemoresistance. To further investigate this association, we systematically evaluated the role of SLC44A1 in modulating drug sensitivity using two clinically relevant agents: cytarabine (a conventional chemotherapeutic drug) and venetoclax (a novel targeted therapy and one of the most frequently prescribed agents in AML treatment). Functional assays demonstrated that SLC44A1 downregulation significantly enhanced the sensitivity of both THP1 and MV4-11 cells to these therapeutic agents (Figures 2A–2D). Consistently, apoptosis assays further confirmed that SLC44A1 downregulation enhanced the sensitivity of THP-1 and MV4-11 cells to both cytarabine and venetoclax, further validating its role in therapeutic resistance (Figures 2E, 2F). These findings indicated that SLC44A1 plays a critical role in modulating therapeutic resistance in AML.

SLC44A1 affects AML progression through the NOTCH signaling pathway. To explore the underlying mechanisms by which SLC44A1 influences AML malignancy, we analyzed the gene expression profile of SLC44A1 knockdown cells using RNA-seq. Based on the RNA-sequencing data, we found that 573 genes were upregulated and 1,251 genes were downregulated in SLC44A1 MV4-11 cell lines (Figure 3A). The list of the top 100 significantly upregulated and downregulated genes has been provided in Supplementary data 1. Gene Ontology (GO) enrichment analysis demonstrated that SLC44A1 is significantly enriched in cellular response to chemical stimulus (Figure 3B), providing a potential mechanistic explanation for its role in chemoresistance. Furthermore, SLC44A1 was found to be involved in critical cellular signaling transduction processes, particularly in cell surface receptor signaling pathways and regulation of signaling (Figure 3B). These findings prompted us to perform KEGG pathway enrichment analysis, which identified the NOTCH signaling pathway as a critical mediator of SLC44A1-driven AML pathogenesis. Subsequent experimental validation revealed that this pathway is associated with the anti-leukemic effects of SLC44A1 knockdown (Figure 3C). Previous studies have shown that activation of the NOTCH pathway induces tumorigenesis

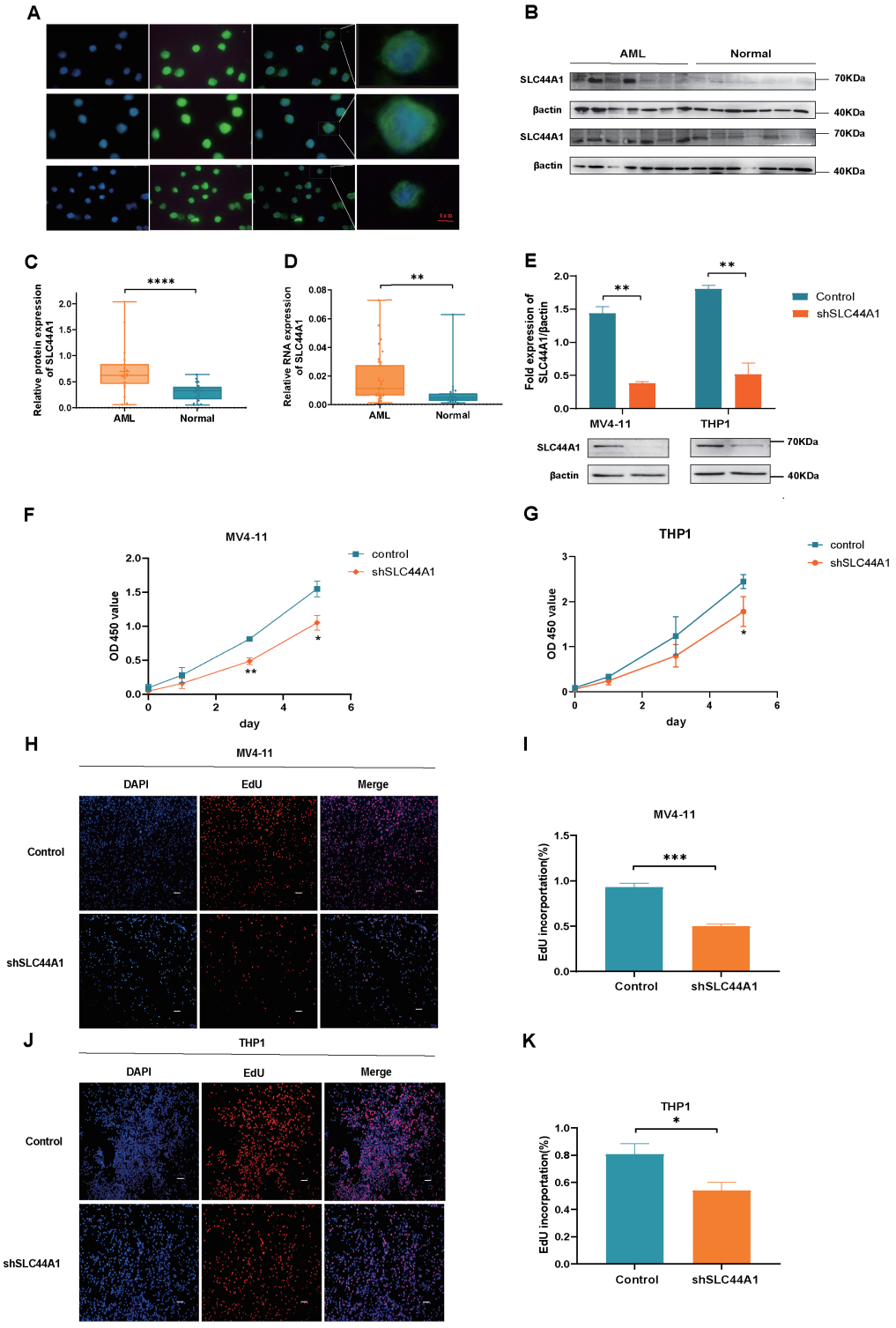

Figure 1. Effects of SLC44A1 knockdown on the proliferation of AML cells. A) Immunofluorescence staining confirmed the subcellular localization of SLC44A1 in AML cell lines (THP-1 and MV4-11) and primary AML samples. B) The expression of SLC44A1 was validated in the AML patients and normal subjects by western blot, and the relative protein level of SLC44A1 was analyzed by ImageJ (C). D) The mRNA level of SLC44A1 in the AML patients and healthy donors was detected by qRT-PCR. E) Knockdown efficiency of SLC44A1 by shSLC44A1 in MV4-11 and THP1 cells. The CCK-8 analyses revealed that the SLC44A1 knockdown caused a significant reduction in MV4-11 (F) and THP1 (G) cell proliferation (the initial number of cultured cells was 2×10^3/well). H–K) The EdU incorporation test suggested that the inhibition of SLC44A1 weakened MV4-11 (H, I) and THP1 (J, K) cell growth (scale bar 200 μm). All experiments were repeated three times independently. Data were analyzed using a two-tailed Student's t-test (F, G, I, K). *p<0.05; **p<0.01; ***p<0.001

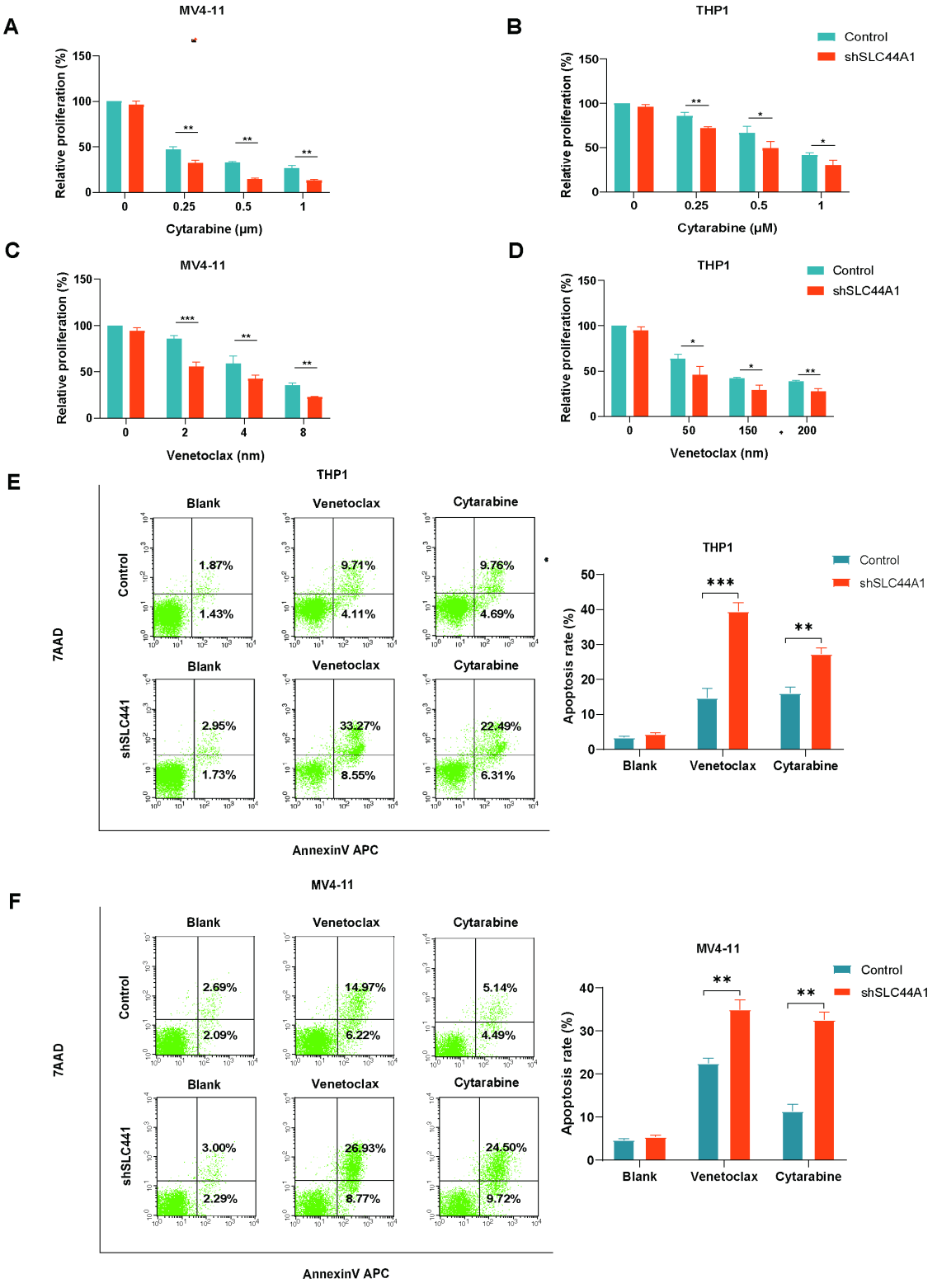

Figure 2. SLC44A1 knockdown enhanced chemosensitivity of AML cells. A, B) The proliferation of SLC44A1-knockdown THP-1 (A) and MV4-11(B) cell lines was assessed following the treatment with cytarabine. C, D) The proliferation of SLC44A1-knockdown THP-1 (C) and MV4-11 (D) cell lines was assessed following treatment with venetoclax. E, F) Cell apoptosis was detected by 7-ADD/Annexin V staining after 24 h of treatment with cytarabine (0.1 μM for MV4-11, 0.2 μM for THP1) and venetoclax (2 nM for MV4-11, 50 nM for THP1). All experiments were repeated three times independently. Data were analyzed using a two-tailed Student's t-test (A–F). *p<0.05; **p<0.01; ***p<0.001

and progression in AML [23]. Subsequently, we compared the expression levels of NOTCH pathway-related proteins between SLC44A1-knockdown AML cells and the control, as NOTCH2 and APH1A were the most significantly affected targets identified in the RNA-seq analysis. Both NOTCH2 and APH1A were significantly downregulated in SLC44A1 knockdown cells (Figures 3D–3F). These results suggested that SCL44A1 promotes AML cell proliferation and drug resistance by regulating the NOTCH signaling pathway, highlighting a potential mechanism underlying SLC44A1-mediated AML malignancy.

Discussion

Despite the development of novel therapies over the past decades, the prognosis for adult AML patients remains poor, especially for those over 65 years old, with a 5-year OS rate of only 30% [24]. Thus, a deeper understanding of the molecular mechanisms underlying AML pathogenesis and the identification of novel therapeutic targets are essential for advancing targeted therapies. This study found that SLC44A1 is highly expressed in adult AML patients compared to healthy donors and is associated with poor clinicopathological features. Furthermore, SLC44A1 exhibited excellent diagnostic value and was linked to an unfavorable prognosis. Based on the functional analysis for SLC44A1, we found that SLC44A1 knockdown inhibited the proliferation of AML cells and enhanced chemosensitivity, highlighting its potential as a therapeutic target in AML.

While SLC44A2 has been documented as a prognostic marker in AML based on the UALCAN [25] database (https://ualcan.path.uab.edu/), the clinical relevance of SLC44A1 in AML remains largely undefined. To address this gap, we systematically evaluated the relationship between SLC44A1 expression and disease outcomes in AML. Our results reveal that high SLC44A1 expression is significantly associated with adverse risk stratification, co-occurrence of poor-prognosis genetic alterations, and shorter OS and EFS. Collectively, these data support the potential utility of SLC44A1 as a prognostic biomarker in AML. Consistently, in BC, SLC44A1 was significantly linked to OS, PFS, and an increased risk of bone metastasis [26]. Additionally, in HNC, SLC44A1 showed higher expression in high-grade (III/IV) tumors compared to low-grade (I/II) tumors [27]. Expression of SLC44A1 was significantly correlated with disease-specific survival (DSS) and PFS. A large-scale analysis involving approximately 2,000 multiple myeloma patients confirmed its correlation with poor prognosis [28],

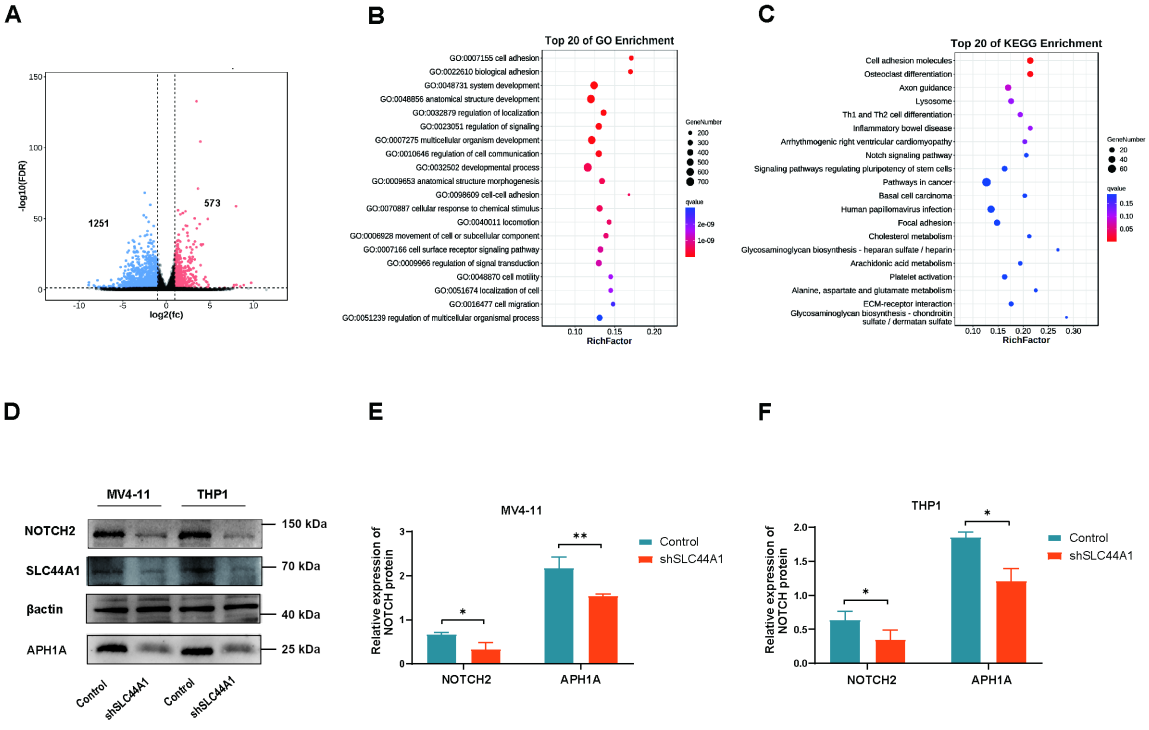

Figure 3. Transcriptomic profiling and pathway analysis in MV4-11 cells after SLC44A1 knockdown. A) The illustration of the Volcano plot showed the change in the gene expression profile in SLC44A1 knockdown AML cells. B) Gene Ontology (GO) enrichment analysis of SLC44A1 targets. C) Kyoto Encyclopedia of Genes and Genomes (KEGG) analysis of identified targets. D) The protein expression level of the NOTCH signaling pathway was detected by western blot. All experiments were repeated three times independently. Data were analyzed using a two-tailed Student's t-test (E, F). *p<0.05; **p<0.01

suggesting that SLC44A1 may serve as a potential biomarker for disease progression and unfavorable clinical outcomes in MM patients. To further establish the prognostic value of SLC44A1 in AML, studies involving large clinical cohorts are required.

In this study, we investigated the role of SLC44A1 in AML cell proliferation and chemosensitivity. Choline is an essential nutrient involved in multiple biological processes, including the synthesis of the membrane lipid phosphatidylcholine (PtdCho) [29]. Dysregulated choline metabolism is a well-established hallmark of proliferation drug resistance and has been implicated in various cancer types [30, 31]. Notably, as a choline transporter, SLC44A1 has been implicated in the increased synthesis of the membrane PtdCho, which is associated with drug resistance in both rectal and pancreatic cancers [32, 33]. Therefore, SLC44A1-mediated AML malignant progression may be regulated by choline metabolism. Resistance to cytarabine and venetoclax in AML involves complex and multifactorial mechanisms. Cytarabine resistance may arise not only from impaired cellular uptake due to reduced expression of nucleoside transporters such as hENT1 and hCNT1, altered mitochondrial metabolism characterized by decreased oxidative phosphorylation, or enhanced DNA repair capacity, but also from dysregulated signaling pathways and adaptations within the tumor microenvironment [34–37]. In contrast, resistance to venetoclax is frequently driven by the upregulation of anti-apoptotic proteins (e.g., MCL-1, BCL-XL), mutations in BAX, or activation of oncogenic pathways such as N/KRAS, FLT3-ITD, and TP53 [38–40]. To our knowledge, this is the first study to demonstrate that downregulation of SLC44A1 enhances the chemosensitivity of AML cells, addressing a critical gap in the current literature. Our findings suggest that SLC44A1 may represent one of the contributing factors to such resistance; however, its precise mechanistic role and significance within the broader resistance network warrant further elucidation through additional *in vitro* and *in vivo* studies.

The observed suppression of AML cell proliferation and enhanced chemosensitivity following SLC44A1 knockdown merit a mechanistic investigation. Our data suggest that this phenotype may be mediated through inhibition of the NOTCH signaling pathway, as evidenced by the concomitant downregulation of key NOTCH-related proteins. Furthermore, SLC44A1 knockdown in AML cells significantly reduced the expression of NOTCH pathway components (NOTCH2 and APH1A), while NOTCH agonist treatment partially reversed the phenotypic effects of SLC44A1 knockdown. NOTCH is an important signaling pathway in cancer, playing a vital role in tumor initiation and progression [41, 42]. Importantly, activation of the NOTCH signaling pathway triggered abnormal leukemic stem cell activation, promoting tumor proliferation and drug resistance [43–45], while downregulation of NOTCH2 has been shown to inhibit AML proliferation [46]. Furthermore, NOTCH activation stimulates bone marrow mesenchymal stromal cells to facilitate AML progression and confer resistance to chemotherapy [47]. As a component of the plasma membrane, the Notch receptor plays a crucial role in activating the NOTCH signaling pathway [48]. Intriguingly, SLC44A1, which our GO analysis identified as being enriched in cell surface receptor signaling pathways, has been implicated in plasma membrane biosynthesis [49]. These findings collectively suggest that SLC44A1 may regulate AML proliferation and drug resistance by modulating the NOTCH receptor or membrane integration, thereby influencing NOTCH signaling activation.

In conclusion, this study identifies SLC44A1 as a key driver of AML pathogenesis and highlights its potential as both a prognostic biomarker and a therapeutic target. Future research should focus on deciphering the downstream signaling pathways regulated by SLC44A1 and its interactions with other oncogenic drivers in AML. Additionally, investigating the therapeutic efficacy of SLC44A1 inhibitors in preclinical AML models will be essential for advancing targeted treatment strategies.

Supplementary information is available in the online version of the paper.

Acknowledgments: The TCGA, GEO (Accession: GSE103424, GSE116256), and GTEx data used for bioinformatics analysis are accessible through their respective portals. The datasets generated during the current study are available in the National Center for Biotechnology Information (NCBI) repository, [BioProject ID PRJNA1223631]. This work was supported by the National Natural Science Foundation of China (82170168, 82370168, 82260728); the Guizhou Provincial Basic Research Program (Natural Science) (Qian Ke He-ZK [2023] No.382); the Foundation the Translational Research Grant of NCRCH (2021WWB01); and the Cultivation Project of National Natural Science Foundation of Guizhou Medical University (Academic new seedlings) (20NSP027, Gyfynsfc-2021-3).

References

[1] SHIMONY S, STAHL M, STONE RM. Acute myeloid leukemia: 2023 update on diagnosis, risk-stratification, and management. Am J Hematol 2023; 98: 502–526. https://doi.org/10.1002/ajh.26822

[2] FORSBERG M, KONOPLEVA M. Aml treatment: conventional chemotherapy and emerging novel agents. Trends Pharmacol Sci 2024; 45: 430–448. https://doi.org/10.1016/j.tips.2024.03.005

[3] BHANSALI RS, PRATZ KW, LAI C. Recent advances in targeted therapies in acute myeloid leukemia. J Hematol Oncol 2023; 16: 29. https://doi.org/10.1186/s13045-023-01424-6

[4] SONG T, ZHAO S, LUO S, CHEN C, LIU X et al. Slc44a2 regulates vascular smooth muscle cell phenotypic switching and aortic aneurysm. J Clin Invest 2024; 134: e173690. https://doi.org/10.1172/JCI173690

[5] HIRAI K, WATANABE S, NISHIJIMA N, SHIBATA K, HASE A et al. Molecular and functional analysis of choline transporters and antitumor effects of choline transporter-like protein 1 inhibitors in human pancreatic cancer cells. Int J Mol Sci 2020; 21: 5190. https://doi.org/10.3390/ijms21155190

[6] GLUNDE K, BHUJWALLA ZM, RONEN SM. Choline metabolism in malignant transformation. Nat Rev Cancer 2011; 11: 835–848. https://doi.org/10.1038/nrc3162

[7] HE J, WANG A, ZHAO Q, ZOU Y, ZHANG Z et al. Rnai screens identify hes4 as a regulator of redox balance supporting pyrimidine synthesis and tumor growth. Nat Struct Mol Biol 2024 2024; 31: 1413–1425. https://doi.org/10.1038/s41594-024-01309-3

[8] FAGERBERG CR, TAYLOR A, DISTELMAIER F, SCHRODER HD, KIBAEK M et al. Choline transporter-like 1 deficiency causes a new type of childhood-onset neurodegeneration. Brain 2020; 143: 94–111. https://doi.org/10.1093/brain/awz376

[9] SHIBATA K, NISHIJIMA N, HIRAI K, WATANABE S, YAMANAKA T et al. A novel plant-derived choline transporter-like protein 1 inhibitor, amb544925, induces apoptotic cell death via the ceramide/survivin pathway in tongue squamous cell carcinoma. Cancers (Basel) 2022; 14: 329. https://doi.org/10.3390/cancers14020329

[10] INAZU M, YAMADA T, KUBOTA N, YAMANAKA T. Functional expression of choline transporter-like protein 1 (ctl1) in small cell lung carcinoma cells: a target molecule for lung cancer therapy. Pharmacol Res 2013; 76: 119–131. https://doi.org/10.1016/j.phrs.2013.07.011

[11] INAZU M, HIRAI K, WATANABE S, NISHIJIMA N, SHIBATA K et al. 25p development of new therapeutic drugs for pancreatic cancer targeting choline transporter-like protein 1 (ctl1/slc44a1). Ann Oncol 2020; 31: S8–09. https://doi.org/10.1016/j.annonc.2020.01.044

[12] LI T, FU J, ZENG Z, COHEN D, LI J et al. Timer2.0 for analysis of tumor-infiltrating immune cells. Nucleic Acids Res 2020: W509–514. https://doi.org/10.1093/nar/gkaa407

[13] TANG Z, LI C, KANG B, GAO G, LI C et al. Gepia: a web server for cancer and normal gene expression profiling and interactive analyses. Nucleic Acids Res 2017; 45: W98–102. https://doi.org/10.1093/nar/gkx247

[14] EDGAR R, DOMRACHEV M, LASH AE. Gene expression omnibus: ncbi gene expression and hybridization array data repository. Nucleic Acids Res 2002; 30: 207–210. https://doi.org/10.1093/nar/30.1.207

[15] Chiu Y, Hsiao T, Tsai J, Wang L, Ho T et al. Integrating resistance functions to predict response to induction chemotherapy in de novo acute myeloid leukemia. Eur J Haematol 2019; 103: 417–425. https://doi.org/10.1111/ejh.13301

[16] CANCER GENOME ATLAS RESEARCH NETWORK, WEINSTEIN JN, COLLISSON EA, MILLS GB, SHAW KRM et al. The cancer genome atlas pan-cancer analysis project. Nat Genet 2013; 45: 1113–1120. https://doi.org/10.1038/ng.2764

[17] GTEX CONSORTIUM. Human genomics. The genotype-tissue expression (gtex) pilot analysis: multitissue gene regulation in humans. Science (New York, N.Y.); 348: 648–60. https://doi.org/10.1126/science.1262110

[18] VASAIKAR SV, STRAUB P, WANG J, ZHANG B. Linkedomics: analyzing multi-omics data within and across 32 cancer types. Nucleic Acids Res 2018; 46: D956–963. https://doi.org/10.1093/nar/gkx1090

[19] VAN GALEN P, HOVESTADT V, WADSWORTH II MH, HUGHES TK, GRIFFIN GK et al. Single-cell rna-seq reveals aml hierarchies relevant to disease progression and immunity. Cell 2019; 176: 1265–1281. https://doi.org/10.1016/j.cell.2019.01.031

[20] GÍSLASON MH, DEMIRCAN GS, PRACHAR M, FURTWÄNGLER B, SCHWALLER J et al. Bloodspot 3.0: a database of gene and protein expression data in normal and malignant haematopoiesis. Nucleic Acids Res 2024; 52: D1138–1142. https://doi.org/10.1093/nar/gkad993

[21] MROZEK K, KOHLSCHMIDT J, BLACHLY JS, NICOLET D, CARROLL AJ et al. Outcome prediction by the 2022 european leukemianet genetic-risk classification for adults with acute myeloid leukemia: an alliance study. Leukemia 2023; 37: 788–798. https://doi.org/10.1038/s41375-023-01846-8

[22] FALINI B, DILLON R. Criteria for diagnosis and molecular monitoring of npm1-mutated aml. Blood Cancer Discov 2024; 5: 8–20. https://doi.org/10.1158/2643-3230.BCD-23-0144

[23] RODRIGUES ACBD, COSTA RGA, SILVA SLR, DIAS IRSB, DIAS RB et al. Cell signaling pathways as molecular targets to eliminate aml stem cells. Crit Rev Oncol Hematol 2021; 160: 103277. https://doi.org/10.1016/j.critrevonc.2021.103277

[24] LACHOWIEZ CA, LOGHAVI S, FURUDATE K, MONTALBAN-BRAVO G, MAITI A et al. Impact of splicing mutations in acute myeloid leukemia treated with hypomethylating agents combined with venetoclax. Blood Adv 2021; 5: 2173–2183. https://doi.org/10.1182/bloodadvances.2020004173

[25] CHANDRASHEKAR DS, KARTHIKEYAN SK, KORLA PK, PATEL H, SHOVON AR et al. Ualcan: an update to the integrated cancer data analysis platform. Neoplasia (New York, N.Y.). 2022; 25: 18–27. https://doi.org/10.1016/j.neo.2022.01.001

[26] FAN TD, BEI DK, LI SW. Nomogram models based on the gene expression in prediction of breast cancer bone metastasis. J Healthc Eng 2022; 2022: 8431946. https://doi.org/10.1155/2022/8431946

[27] MA W, CAO Q, SHE W. Identification and clinical validation of gene signatures with grade and survival in head and neck carcinomas. Braz J Med Biol Res 2021; 54: e11069. https://doi.org/10.1590/1414-431X2020e11069

[28] GAROFANO F, CORSALE AM, SHEKARKAR AZGOMI M, DI SIMONE M, SPECIALE M et al. Unveiling novel therapeutic targets for car therapy in multiple myeloma through single-cell rna sequencing. Blood 2023; 142: 6605. https://doi.org/10.1182/blood-2023-188474

[29] MA Q, JIANG H, MA L, ZHAO G, XU Q et al. The moonlighting function of glycolytic enzyme enolase-1 promotes choline phospholipid metabolism and tumor cell proliferation. Proc Natl Acad Sci U S A 2023; 120: e2085532176. https://doi.org/10.1073/pnas.2209435120

[30] WEN S, HE Y, WANG L, ZHANG J, QUAN C et al. Aberrant activation of super enhancer and choline metabolism drive antiandrogen therapy resistance in prostate cancer. Oncogene 2020; 39: 6556–6571. https://doi.org/10.1038/s41388-020-01456-z

[31] RIZZO A, SATTA A, GARRONE G, CAVALLERI A, NAPOLI A et al. Choline kinase alpha impairment overcomes trail resistance in ovarian cancer cells. J Exp Clin Cancer Res 2021 2021; 40: 5. https://doi.org/10.1186/s13046-020-01794-6

[32] ANDREJEVA G, GOWAN S, LIN G, WONG TFA, SHAMSAEI E, et al. De novo phosphatidylcholine synthesis is required for autophagosome membrane formation and maintenance during autophagy. Autophagy 2020; 16: 1044–1060. https://doi.org/10.1080/15548627.2019.1659608

[33] SAITO RF, ANDRADE L, BUSTOS SO, CHAMMAS R. Phosphatidylcholine-derived lipid mediators: the crosstalk between cancer cells and immune cells. Front Immunol 2022; 13: 768606. https://doi.org/10.3389/fimmu.2022.768606

[34] JARAMILLO AC, HUBEEK I, BROEKHUIZEN R, PASTOR-ANGLADA M, KASPERS GJL et al. Expression of the nucleoside transporters hent1 (slc29) and hcnt1 (slc28) in pediatric acute myeloid leukemia. Nucleosides Nucleotides Nucleic Acids 2020; 39: 1379–1388. https://doi.org/10.1080/15257770.2020.1746803

[35] YEON CHAE S, JANG S, KIM J, HWANG S, MALANI D et al. Mechanisms of chemotherapy failure in refractory/relapsed acute myeloid leukemia: the role of cytarabine resistance and mitochondrial metabolism. Cell Death Dis 2025; 16: 331. https://doi.org/10.1038/s41419-025-07653-6

[36] WU J, LI X, LIU Y, CHEN G, LI R et al. Mmp14 from bm-mscs facilitates progression and ara-c resistance in acute myeloid leukemia via the jak/stat pathway. Exp Hematol Oncol 2025; 14: 43. https://doi.org/10.1186/s40164-025-00635-6

[37] SHIVHARE K, SATIJA NK. Acute myeloid leukemia-osteoblast interaction mediated autophagy induction protects against cytarabine induced apoptosis. Cell Biochem Funct 2025; 43: e70055. https://doi.org/10.1002/cbf.70055

[38] WANG Z, LAI R, WANG X, CHEN X, ZHOU Y et al. Targeted penetrating motif engineering of bh3 mimetic: harnessing non-canonical amino acids for coinhibition of mcl-1 and bcl-xl in acute myeloid leukemia. Adv Sci (Weinh) 2025; 12: e2503682. https://doi.org/10.1002/advs.202503682

[39] MOUJALLED DM, BROWN FC, CHUA CC, DENGLER MA, POMILIO G et al. Acquired mutations in bax confer resistance to bh3-mimetic therapy in acute myeloid leukemia. Blood 2023; 141: 634–644. https://doi.org/10.1182/blood.2022016090

[40] LACHOWIEZ CA, HEIBLIG M, ASPAS REQUENA G, TAVERNIER-TARDY E, DAI F et al. Genetic and phenotypic correlates of clinical outcomes with venetoclax in acute myeloid leukemia: the gen-phen-ven study. Blood Cancer Discov 2025; 6: 437–449. https://doi.org/10.1158/2643-3230.BCD-24-0256

[41] ZHOU B, LIN W, LONG Y, YANG Y, ZHANG H et al. Notch signaling pathway: architecture, disease, and therapeutics. Signal Transduct Target Ther 2022; 7: 95. https://doi.org/10.1038/s41392-022-00934-y

[42] SHI Q, XUE C, ZENG Y, YUAN X, CHU Q et al. Notch signaling pathway in cancer: from mechanistic insights to targeted therapies. Signal Transduct Target Ther 2024; 9: 128. https://doi.org/10.1038/s41392-024-01828-x

[43] TOMASONI C, ARSUFFI C, DONSANTE S, CORSI A, RIMINUCCI M et al. Aml alters bone marrow stromal cell osteogenic commitment via notch signaling. Front Immunol 2023; 14: 1320497. https://doi.org/10.3389/fimmu.2023.1320497

[44] NAEF P, RADPOUR R, JAEGER-RUCKSTUHL CA, BODMER N, BAERLOCHER GM et al. Il-33-st2 signaling promotes stemness in subtypes of myeloid leukemia cells through the wnt and notch pathways. Sci Signal 2023; 16: eadd7705. https://doi.org/10.1126/scisignal.add7705

[45] LAINEZ-GONZALEZ D, SERRANO-LOPEZ J, ALONSO-DOMINGUEZ JM. Understanding the notch signaling pathway in acute myeloid leukemia stem cells: from hematopoiesis to neoplasia. Cancers (Basel) 2022; 14: 1459. https://doi.org/10.3390/cancers14061459

[46] MA X, ZHANG W, ZHAO M, LI S, JIN W et al. Oncogenic role of lncrna crnde in acute promyelocytic leukemia and npm1-mutant acute myeloid leukemia. Cell Death Discov 2020; 6: 121. https://doi.org/10.1038/s41420-020-00359-y

[47] TAKAM KP, BASSI G, CASSARO A, MIDOLO M, DI TRAPANI M et al. Notch signalling drives bone marrow stromal cell-mediated chemoresistance in acute myeloid leukemia. Oncotarget 2016; 7: 21713–21727. https://doi.org/10.18632/oncotarget.7964

[48] MEDINA E, PEREZ DH, ANTFLK D, LUCA VC. New tricks for an old pathway: emerging notch-based biotechnologies and therapeutics. Trends Pharmacol Sci 2023; 44: 934–948. https://doi.org/10.1016/j.tips.2023.09.011

[49] TAYLOR A, GRAPENTINE S, ICHHPUNIANI J, BAKOVIC M. Choline transporter-like proteins 1 and 2 are newly identified plasma membrane and mitochondrial ethanolamine transporters. J Biol Chem 2021; 296: 100604. https://doi.org/10.1016/j.jbc.2021.100604

https://doi.org/10.4149/neo_2025_250518N209

SLC44A1 promotes AML progression and chemoresistance by regulating the Notch signaling pathway

Shuyun CAO[1,2,3], Chengyun PAN[1,3], Xiuying HU[1,2,3], Tianzhen HU[1,3,4], Yanju LI[1,3], Qin FANG[5], Jishi WANG[1,2,3,4,6,*]

Supplementary Information

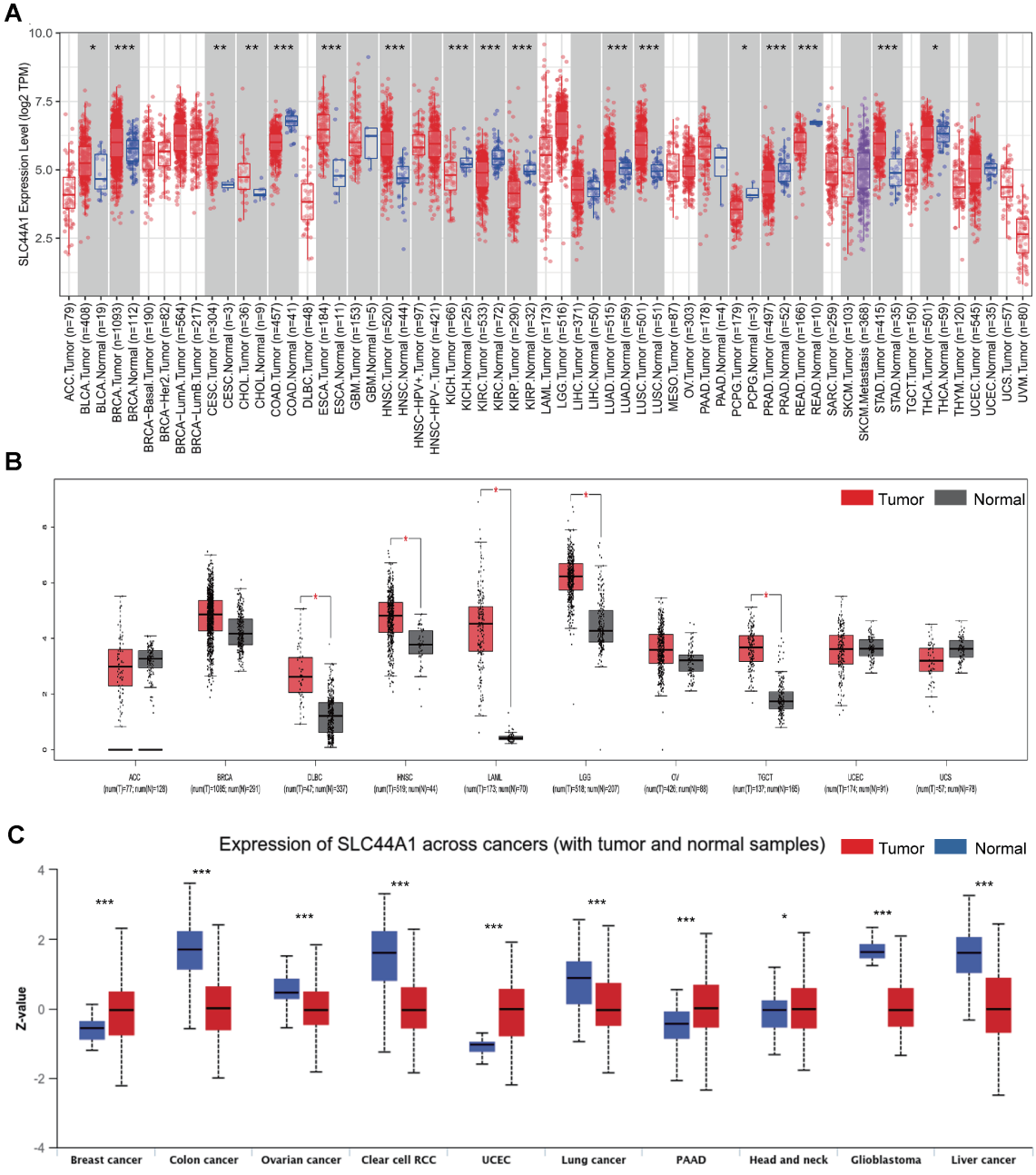

Supplementary Figure S1. SLC44A1 expression in Pan-Cancer. A) SLC44A1 expression levels in 33 tumor types and normal tissues from the TCGA database. B) For tumors lacking normal tissue data in TCGA, SLC44A1 expression was compared between tumor tissues and matched normal tissues from the GTEx database using GEPIA. C) The UALCAN database was applied to compare SLC44A1 protein expression between tumor and respective normal tissues. *p<0.05; **p<0.01; ***p<0.001; ****p<0.0001

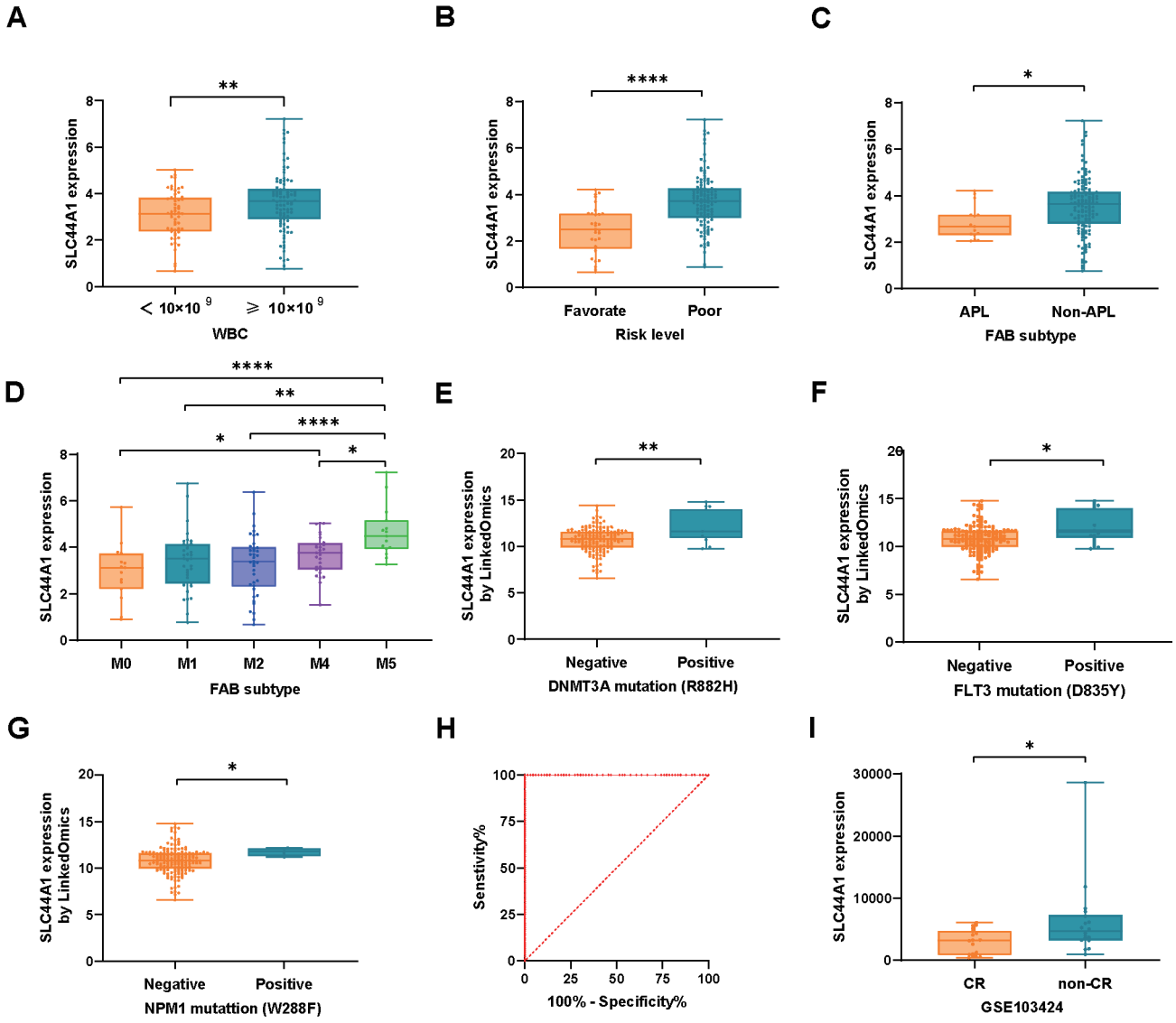

Supplementary Figure S2. Clinical Relevance of SLC44A1 in AML. A–D) Association of SLC44A1 expression with WBC count (A), risk level (B), APL subtype (C), and FAB classification (M0, M1, M2, M4, M5) (D) was analyzed in the TCGA cohort. E–G) The expression level of SLC44A1 was detected in the AML patients with DNMT3A mutation (R882H) (E), FLT3 mutation (D835Y) (F), and NPM1 mutation (W288F) (G) by LinkedOmics. H) The ROC curve for SLC44A1 in the AML and normal subjects from TCGA. (I) SLC44A1 expression in GSE103424. Data were analyzed using the Mann-Whitney U test (A–C, E–G, I), and one-way ANOVA (D). *p<0.05; **p<0.01; ***p<0.001; ****p<0.0001

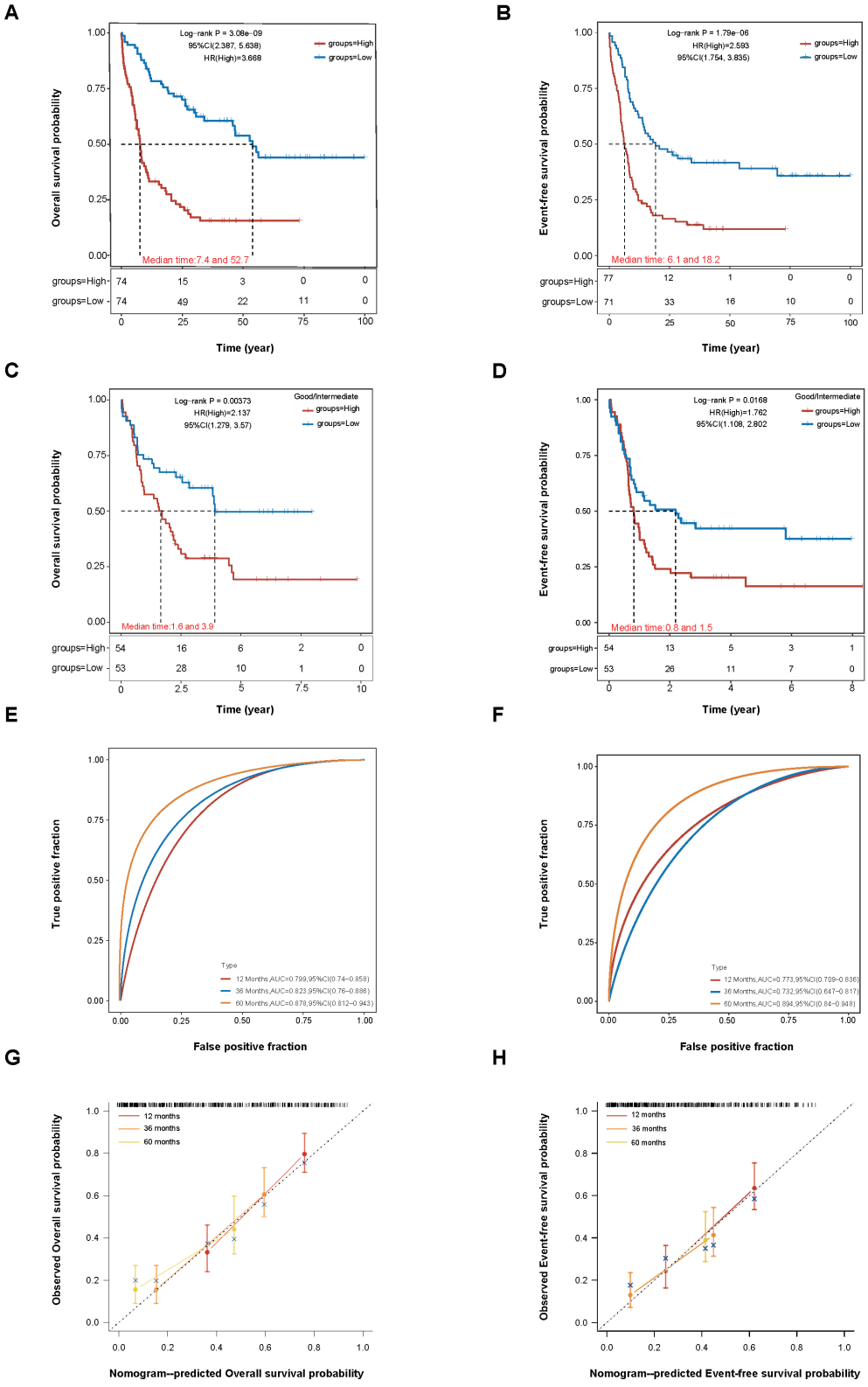

Supplementary Figure S3. SLC44A1 predicts poor prognosis in AML. A, B) Kaplan-Meier survival analysis for overall survival (OS) (A) and event-free survival (EFS) (B) based on the TCGA cohort. C, D) Kaplan-Meier curves for OS (C) and EFS (D) in good/intermediate-risk subsets from the TCGA cohort. E, F) The ROC curve and AUC value of a nomogram for OS (E) and EFS (F). G, H) Calibration plots of the nomogram for 1-, 3-, and 5-years OS (G), calibration plots of the nomogram for 1-,3-, and 5-years EFS (H). Data were analyzed using Kaplan-Meier (KM) analysis (A–D).

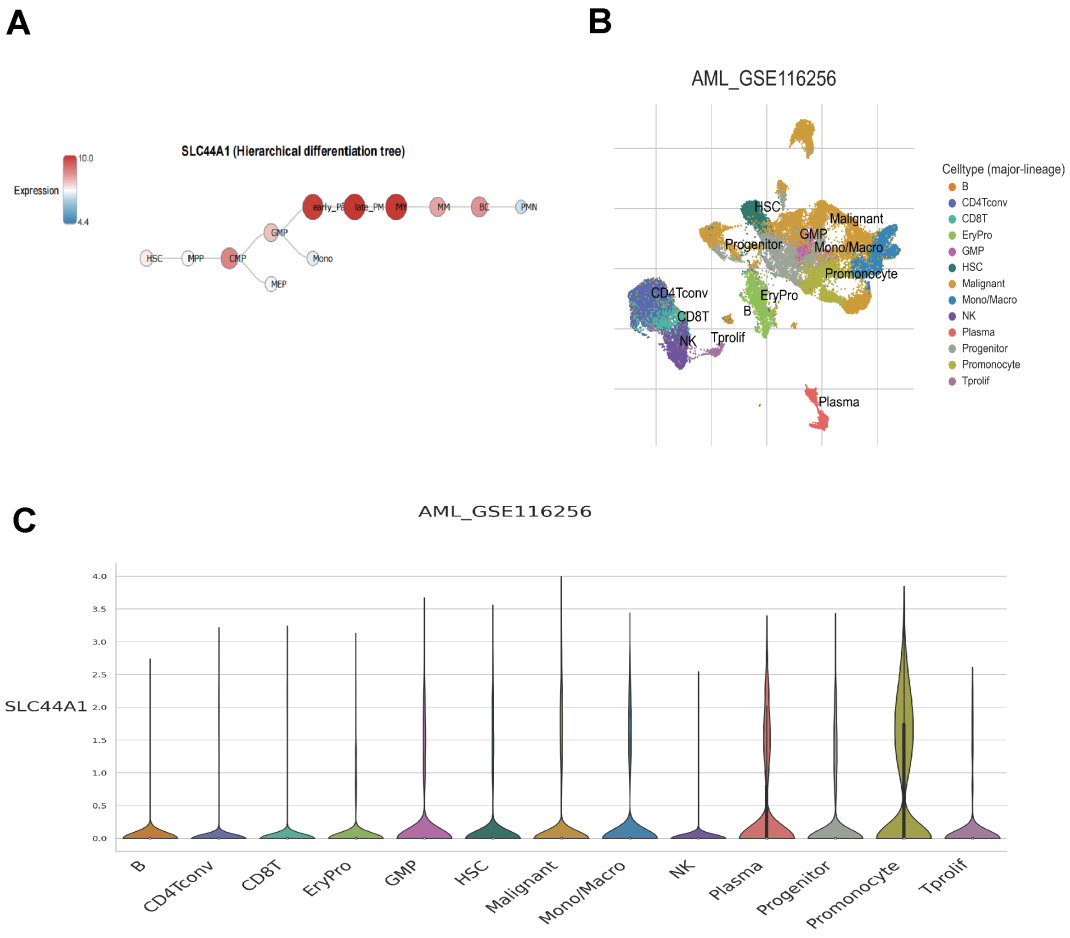

Supplementary Figure S4. Integrated Single-cell and Immunofluorescence Mapping of SLC44A1 in AML. A) Expression of SLC44A1 during hematopoietic differentiation. B, C) Single-cell RNA sequencing analysis revealed distinct SLC44A1 expression patterns across immune cell populations.

Supplementary Table S1. Characteristics of patient samples.

Patients no.	Age (years)	Gender	FAB subtype	Cell count ($\times 10^9$)			BM Blast (%)	Karyotype
				WBC	Hb	PLT		
1	55	M	M2	28.28	111	7	40	46, XX
2	61	M	M2	39.02	59	87	57	46, XX
3	37	F	M2	22.4	50	5	74	46, XY t(8:21)
4	50	F	M2	28.92	75	6	48	Complex karyotype
5	76	F	M4	77.79	84	16	56	46, XY del(4)
6	51	M	M5	168.25	84	21	87	46, XX
7	76	F	M5	284.06	96	33	95	46, XY
8	79	M	M4/M5	147.07	113	38	78	46, XX
9	69	M	M2	72.28	114	66	89	46, XX
10	55	F	M2	8.57	47	14	21	46, XY t(8:21)
11	70	F	M5	234.85	79	27	77	46, XY
12	20	M	M4	142.94	85	37	92	46, XX der(11)
13	82	F	M2	2.33	70	25	27	46, XY
14	78	M	M4	26.68	89	344	72	46, XX